Polarization and Surface Roughness Effects on Equilibrium Temperature for Interacting Surfaces

T. F. Smith,* T. K. Kim,† and P. Hix†
University of Iowa, Iowa City, Iowa

Theoretical analyses and results are presented to examine polarization and surface roughness effects on equilibrium temperature acquired by interacting surfaces in the presence of a uniform, collimated solar flux. A semigray spectral model is employed to account for surface properties that differ for the solar spectral interval and wavelengths for surface or thermal emission. The surfaces are composed of V-shaped roughness elements with a characteristic length larger than the solar wavelengths. Element walls are optically smooth with directional specular reflectance given by electromagnetic theory for the parallel and perpendicular polarized components. The roughness is discussed in terms of a root-mean-square slope. For surface emission, the surfaces are diffusely emitting and specularly reflecting with a constant specular reflectance. Results are also presented for less detailed surface property models for the solar wavelengths. The interacting surfaces consist of an adjoint plate system where representative results are reported for an included angle of 90 deg. Comparisons of results from the various property models reveal that polarization effects can be neglected and it is more important to account for the directional variation of the properties.

Nomenclature

G	= absorbed solar irradiation
$\mathcal{G}$	= dimensionless absorbed solar irradiation, G/S
H	= dimensionless solar intensity, $I^+/(S/\pi)$
I^-, I^+	= intensity of incident and emergent solar energy
L	= plate length
m	= root-mean-square slope
n	= refractive index
$\bar{R}$	= ratios of reflected energy
S	= solar constant
T	= temperature
x,y	= coordinates
α_d	= directional absorptance
α_h	= hemispherical absorptance
α_w	= roughness element wall solar absorptance
γ	= included angle
ϵ	= hemispherical emittance
Θ	= dimensionless temperature, $T/(S/\sigma)^{1/4}$
θ', θ	= polar angle of incident and emergent solar energy
κ	= extinction coefficient
ζ, η	= dimensionless coordinates, x/L, y/L
ρ	= solar reflectance
ρ_s	= specular component of solar reflectance
ρ_{bd}	= bidirectional reflectance
σ	= Stefan-Boltzmann radiation constant
χ	= roughness element included angle
$d\omega', d\omega$	= solid angles of incident and emergent energy

Subscripts

p	= parallel polarized component
s	= perpendicular polarized component

Introduction

A BIDIRECTIONAL reflectance model[1] was developed to examine polarization and surface roughness effects on the magnitude and spatial distribution of reflected radiant energy. The model demonstrates that polarization effects are more important for dielectric materials than for conducting materials and for shorter wavelengths for both materials. Surface roughness effects are similar to those cited for a previous model[2] which served as the basis for this more extensive model. The earlier model was utilized to examine surface roughness effects on equilibrium temperature for interacting rough surfaces in the presence of a solar flux. It would be of interest, therefore, to examine equilibrium temperature distributions based on a bidirectional reflectance model that includes polarization effects.

Surface roughness effects on equilibrium temperature were reported by Houchens and Hering[3] for slightly rough surfaces with the radiation property model given by the Beckmann model.[4] Hering and Smith[5] and Smith[6] utilized the respective bidirectional reflectance models for identical roughness elements[7] and for randomly distributed roughness elements[2] to examine surface roughness effects on equilibrium temperature when the wavelength of incident solar energy is much smaller than the characteristic length of the roughness elements. In both of these models, a directional independent specular reflectance for the roughness element was employed. The influence of directional property effects on equilibrium temperature for smooth surfaces was examined by Houchens and Hering.[8] In that study, directional dependence of the properties was evaluated from electromagnetic theory.[9] Hering[10] examined equilibrium temperature distributions where a directional independent specular-diffuse reflectance model was considered. In all of these investigations, polarization effects were neglected. Edwards and Bevans,[11] as well as Edwards and Tobin,[12] illustrated methods for including polarization effects in radiative heat transfer studies. Significant errors due to omission of polarization were cited. Extension of these findings to equilibrium temperature results where the fourth root of the absorbed radiant energy must be taken to obtain the temperature remains to be evaluated. The purpose of this study is to utilize the bidirectional reflectance model reported in Ref. 1 to evaluate polarization and surface roughness effects on equilibrium temperature for interacting surfaces in the presence of a solar field and to ascertain the accuracy attained by less detailed radiation surface property models.

The system of radiatively interacting surfaces depicted in Fig. 1 consists of equal length plates of infinite width sharing a common edge with included angle γ. Both surfaces are opaque and adiabatic and exhibit uniform temperature in-

Received Nov. 23, 1981; revision received May 19, 1982.

*Professor, Division of Energy Engineering. Member AIAA.
†Research Assistant, Division of Energy Engineering.

dependent properties. The intervening medium is transparent with unit refractive index. A uniform, unpolarized, and collimated solar flux directed parallel to the bisector of γ irradiates the surface. The system is characteristic of that appearing in several thermal control applications. Equilibrium temperature results for this system are available for some simple property models which neglect surface roughness, directional, and polarization effects[8,10] and for rough surface property models where polarization effects are neglected.[3,5,6] The surfaces are composed of V-shaped roughness elements with axes parallel to the common edge, upper edges lying in a common plane, and a random distribution of included angle χ or slope. A semigray spectral model[10] is employed to describe differences in surface properties for solar energy and surface or thermal emission. Wavelengths of the solar energy are considered small in comparison to the characteristic length of the V-groove roughness elements. The walls of the grooves are taken to be specular reflectors with parallel and perpendicular polarized components given by the directional dependent Fresnel relations.[9] As a result of the orientation and specular walls of the V grooves and the collimated solar field, the reflection phenomenon for solar energy occurs within a plane that is perpendicular to the common edge, and the phase change upon reflection need not be considered.[11] The bidirectional reflectance model reported in Ref. 1, therefore, can be employed to provide rough surface properties for the solar spectral interval. Attention is directed at the properties for surface emission. It is known that as the wavelength increases, a rough surface approaches a specular reflector[13] and polarization effects diminish.[1] Houchens and Hering[8] presented equilibrium temperature results that illustrate small differences between directional dependent and independent thermal property models. Based on these findings, the surfaces are assumed to be optically smooth with a directional independent specular reflectance model employed to describe reflection of emitted energy. A diffuse model is utilized for surface emission.

Analysis

Analysis of radiant exchange for the interacting rough surfaces and for the radiation property model employed to describe bidirectional reflectance for the solar spectrum yields expressions similar to those reported elsewhere, with the exception that polarization effects must be accounted for in the solar spectral interval. Consequently, only the final form of the governing expressions are cited with further details of the derivations found in Ref. 5. Local dimensionless equilibrium temperature is expressed by the following integral equation

$$\Theta^4(\zeta) = \frac{1}{\epsilon}\mathcal{G}(\zeta) + \epsilon\int_0^1 \Theta^4(\eta)K_\gamma(\zeta,\eta)\,d\eta \tag{1}$$

where $\mathcal{G}(\zeta)$ is the absorbed solar energy. The exchange factor for surface emission $K_\gamma(\zeta,\eta)$ is available for included angles

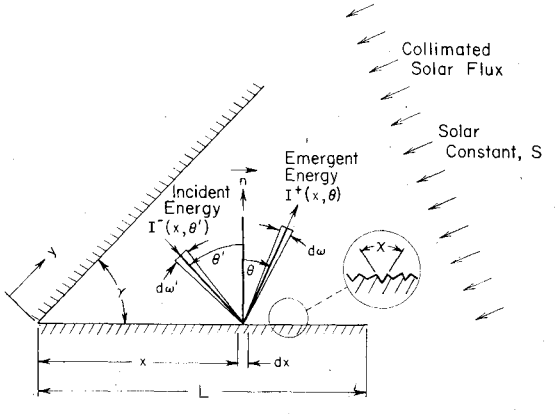

Fig. 1 Schematic diagram of adjoint plate system.

$\gamma = \pi/n$, where n is a positive integer, as

$$K_\gamma(\zeta,\eta) = \sum_{j=1}^{M}(1-\epsilon)^{j-1}f_{j\gamma}(\zeta,\eta) \tag{2}$$

where

$$f_{j\gamma}(\zeta,\eta) = \frac{\zeta\eta\sin^2 j\gamma}{2(\zeta^2+\eta^2-2\zeta\eta\cos j\gamma)^{3/2}} \tag{3}$$

and $M = n-1$. Dimensionless locally absorbed solar energy is evaluated from

$$\mathcal{G}(\zeta) = \mathcal{G}_p(\zeta) + \mathcal{G}_s(\zeta) \tag{4}$$

where subscripts p and s denote the parallel and perpendicular polarized components, respectively. The parallel component of the absorbed solar energy is evaluated from

$$\mathcal{G}_p(\zeta) = \frac{1}{2}\alpha_{dp}(\theta_s')\sin\frac{\gamma}{2} + \frac{1}{2}\int_{\theta'_{\lim(\zeta)}}^{\pi/2}\alpha_{dp}(\theta')\times H_p[\eta(\zeta,\theta'),\phi(\theta')]\cos\theta'\,d\theta' \tag{5}$$

where the first term in Eq. (5) accounts for directly incident absorbed solar energy with $\alpha_{dp}(\theta')$ representing the parallel component of directional absorptance for polar angle of incidence of θ'. The absorbed solar energy attributed to solar intensity leaving the adjacent plate is described by the second term of Eq. (5). Dimensionless solar intensity emerging from the plate at position ζ into the θ direction for the p component is

$$H_p(\zeta,\theta) = \frac{\pi}{2}\rho_{bd,p}(\theta_s',\theta)\sin\frac{\gamma}{2} + \frac{\pi}{2}\int_{\theta'_{\lim(\zeta)}}^{\pi/2}\rho_{bd,p}(\theta',\theta)\times H_p[\eta(\zeta,\theta'),\phi(\theta')]\cos\theta'\,d\theta' \tag{6}$$

where $\rho_{bd,p}(\theta',\theta)$ is the parallel component of the rough surface bidirectional reflectance. In Eqs. (5) and (6), θ_s' $[=(\pi-\gamma)/2]$ is the polar angle of incidence for directly incident solar energy. The factor of one-half in the first term of Eqs. (5) and (6) is due to the directly incident solar energy assumed to be unpolarized. Expressions for $G_s(\zeta)$ and $H_s(\zeta,\theta)$ are obtained from Eqs. (5) and (6), respectively, by substitution of subscript s for p. When polarization effects are neglected, the factor of one-half is replaced by unity and only one each of the absorbed solar energy and solar intensity expressions is required. For the adjoint plate system, contributing directions for solar energy emerging from the adjacent plate are limited to a value of $\theta'_{\lim(\zeta)}$ given by

$$\theta'_{\lim(\zeta)} = -\tan^{-1}[(\cos\gamma-\zeta)/\sin\gamma] \tag{7}$$

From geometry, it follows that

$$\eta = \frac{\zeta\cos\theta'}{\cos(\theta'-\gamma)} \quad \text{and} \quad \phi' = \theta'-\gamma \tag{8}$$

Expressions are presented elsewhere[10] for equilibrium temperature in which all directional and polarization dependencies of radiation properties are ignored. The numerical method employed to solve the integral equations for local solar intensity and equilibrium temperature is described in Ref. 5.

Radiation Property Models

The purpose of this discussion is to examine some characteristics of radiation property models employed in this study for the solar spectral interval. The rough surface property model for the solar spectrum is discussed in detail elsewhere[1] and only a brief examination of the model is

presented. The model was developed for a one-dimensional rough surface composed of V-shaped roughness elements with randomly distributed slopes characterized by root-mean-square (rms) slope m. Roughness element walls were taken as specularly reflecting, with directional dependent polarization components specified by the Fresnel relations.[9] The material properties are given by the complex refractive index $\tilde{n}=n-i\kappa$ where n and κ are the optical constants of refractive index and extinction coefficient, respectively. Multiple reflections and shadowing effects are accounted for accurately in the model. Some representative bidirectional reflectance distributions for the parallel, perpendicular, and mixed components are illustrated in Fig. 2, whereas Table 1 presents rough surface directional absorptances for several values of rms slope and for a polar angle of directly incident solar energy equal to 45 deg. $\bar{R}$ in Fig. 2 represents the ratio of the product of bidirectional reflectance for either parallel, perpendicular, or mixed component and cosine of polar angle of reflection to the corresponding product for the mixed component in the specular direction. The mixed component of bidirectional reflectance is evaluated from the following expression.

$$\rho_{bd}(\theta',\theta) = [\rho_{bd,p}(\theta',\theta) + \rho_{bd,s}(\theta',\theta)]/2 \qquad (9)$$

Table 1 Directional absorptance for directly incident solar energy ($\theta_s' = 45$ deg)

n	κ	m	$\alpha_{d,p}$	$\alpha_{d,s}$	α_d
1.557	0	0.1	0.988	0.893	0.941
		0.4	0.978	0.909	0.944
		1.0	0.972	0.932	0.952
6.1038	0	0.1	0.609	0.375	0.492
		0.4	0.609	0.406	0.514
		1.0	0.601	0.454	0.532
23.452	23.452	0.1	0.114	0.059	0.086
		0.4	0.131	0.065	0.099
		1.0	0.133	0.076	0.105

Results are shown for dielectric ($n=1.557$, $\kappa=0$) and metallic ($n=\kappa=23.452$) materials with $m=0.1$, 0.2, and 0.3 for $\theta'=0$, 30, 60, and 80 deg. The optical constants were selected to yield hemispherical absorptances α_h for smooth surfaces of 0.9 and 0.1 for the dielectric and metallic materials, respectively. This was undertaken in order to facilitate comparisons of rough surface equilibrium temperature results with those from less detailed property models. Polarization effects are more important for the dielectric material and increase as rms slope and polar angle of incidence increase. The presence of peaks in the distributions which appear at polar angles of reflection other than the specular direction where $\theta=\theta'$ can be explained in terms of the Fresnel relations and the presence of the factor of $\cos\theta$ in $\bar{R}$.

Various property models are introduced in order to evaluate polarization and surface roughness effects on equilibrium temperatures. Equilibrium temperature distributions applicable for the rough surface property model with polarization are designated rough surface with polarization (RSP). Distributions for the RSP property model are compared with results based on the mixed component of bidirectional reflectance where directional effects as caused by the directional dependency of specular reflectance for the V-groove walls are included but polarization effects are neglected. These results are denoted as rough surface with mixed component (RSM). Results are also presented for the rough surface property model where a directional independent specular reflectance is employed for the groove walls. These results as reported in Ref. 6 are characterized by a groove wall hemispherical solar absorptance α_w and are referred to as rough surface with constant wall specular reflectance (RSC). In addition to these rough surface property models, results for several less complex property models for smooth surfaces are examined. Two simplified models retain the dependency of hemispherical reflectance on direction of incident energy and consider the reflection to be apportioned between diffuse and specular reflection according to the specularity ratio ρ_s/ρ,

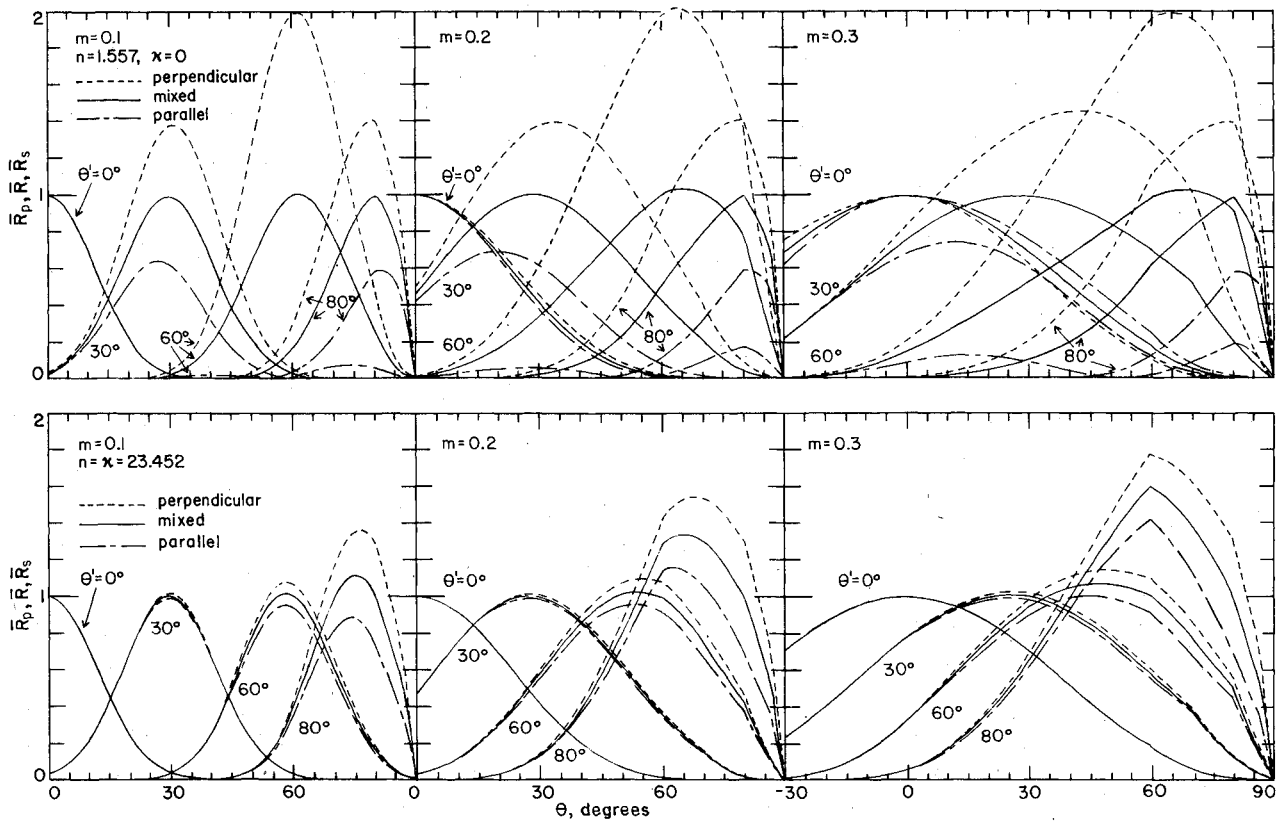

Fig. 2 Bidirectional reflectance distributions.

which is taken to be direction and polarization independent. Furthermore, polarized or mixed components of specular reflectance may be utilized. The two property models which include directional dependence as specified by the Fresnel relations[9] are directional dependent specular plus diffuse with polarization (DSDP) and directional dependent specular plus diffuse with mixed component (DSDM). The DSDM model was employed elsewhere.[3,8] When directional effects are neglected, the DSDM model reduces to the familiar direction independent specular plus diffuse reflection model.[3,8,10] Results derived from this model are referred to as constant property specular plus diffuse (CSD) with apportionment of reflected energy between the specular and diffuse components governed by the specularity ratio. The limiting cases of diffuse and specular reflection are included in the latter three models when $\rho_s/\rho = 0$ and 1, respectively.

Results and Discussion

Solar Intensity

Representative solar intensity distributions for parallel and perpendicular components are presented in Fig. 3 as a function of the polar angle of reflection for rms slopes equal to 0.1 and 0.3. Results are shown for values of optical constants which yield hemispherical absorptances equal to 0.1, 0.5, and 0.9 where the former is characteristic of a conducting material and the latter two are representative of dielectric materials. For hemispherical absorptance of 0.5, the optical constants are $n = 6.1038$ and $\kappa = 0$. For each hemispherical absorptance, distributions are illustrated for spatial positions near the common edge ($\zeta = 0.01$), midpoint of the plate ($\zeta = 0.51$), and outer edge of the plate ($\zeta = 0.99$). Negative values of θ correspond to directions directed into the adjoint plate system. For $m = 0.1$, peaks occurring near $\theta' = -45$ deg are attributed to reflection of directly incident solar energy and are nearly independent of the spatial position along the plates. For positive values of θ, peaks are found at values of θ other than for specularly reflecting plates where a peak due to twice reflected solar energy exists at $\theta = 45$ deg. It is interesting to note that solar intensity is essentially zero within the vicinity of the mean surface normal where $\theta = 0$ deg. For $m = 0.3$, significant scattering of reflected energy occurs as indicated by bidirectional reflectance distributions in Fig. 2 and solar intensity distributions exhibit a near diffuse behavior characterized by a nearly constant value for all values of θ. In all instances, the perpendicular component for solar intensity is larger than that for the parallel component and the difference between the parallel and perpendicular distributions is maximum for $\alpha_h = 0.5$. The magnitude of solar intensity decreases with increasing hemispherical absorptance, and the parallel component is almost negligible for $\alpha_h = 0.9$.

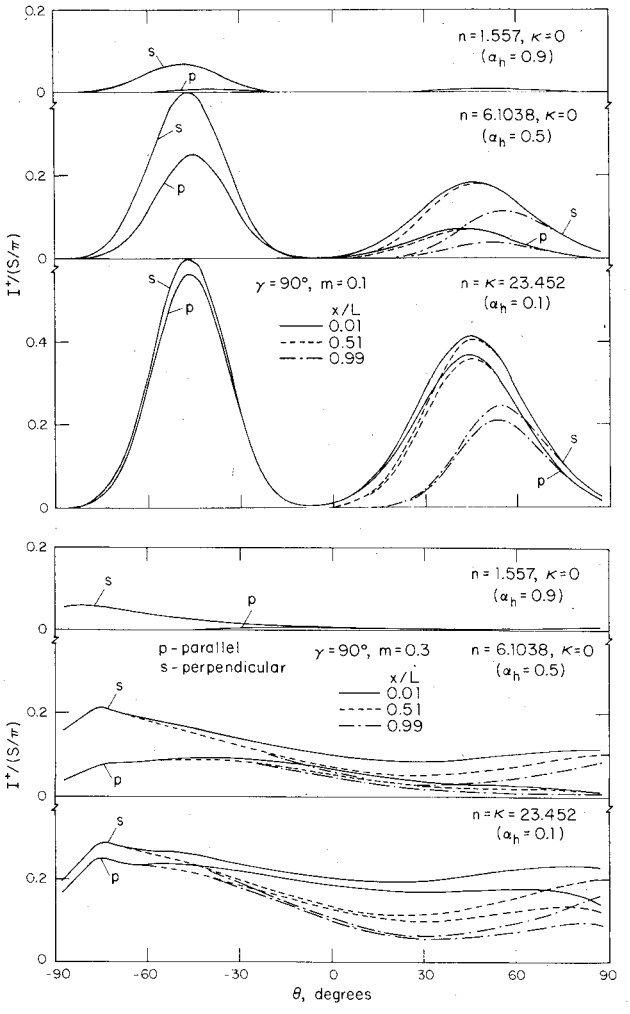

Fig. 3 Solar intensity distributions.

Equilibrium Temperature

Representative equilibrium temperature distributions for radiation properties for the solar spectral interval evaluated from the rough surface property model with polarization (RSP) are shown in Figs. 4-8 for an included angle of 90 deg. Results for hemispherical emittance of 0.1 are presented in Figs. 4, 5, and 6 for hemispherical absorptances of 0.1, 0.5, and 0.9, respectively. The optical constants which yield hemispherical absorptances of 0.1, 0.5, and 0.9 for uniform irradiation are $n = \kappa = 23.452$; $n = 6.1038$, $\kappa = 0.0$; and $n = 1.557$, $\kappa = 0.0$, respectively. In Figs. 7 and 8, distributions for hemispherical emittance of 0.9 are illustrated for hemispherical absorptances of 0.1 and 0.5, respectively. Distributions not displayed for hemispherical emittance and absorptance of 0.9 nearly coincide for the RSP, RSM, DSDP, and DSDM property models and range from $T/\sqrt[4]{S/\sigma} = 1.095$ at the apex to 0.965 at the outer edge. The general character of rough surface equilibrium temperature distributions for the adjoint plate system is similar to that discussed elsewhere[6]

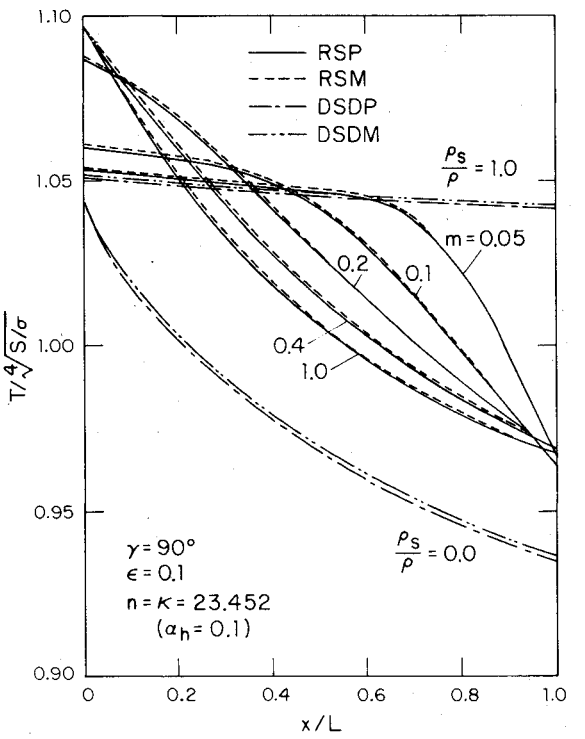

Fig. 4 Equilibrium temperature for $\epsilon = 0.1$, $\alpha_h = 0.1$.

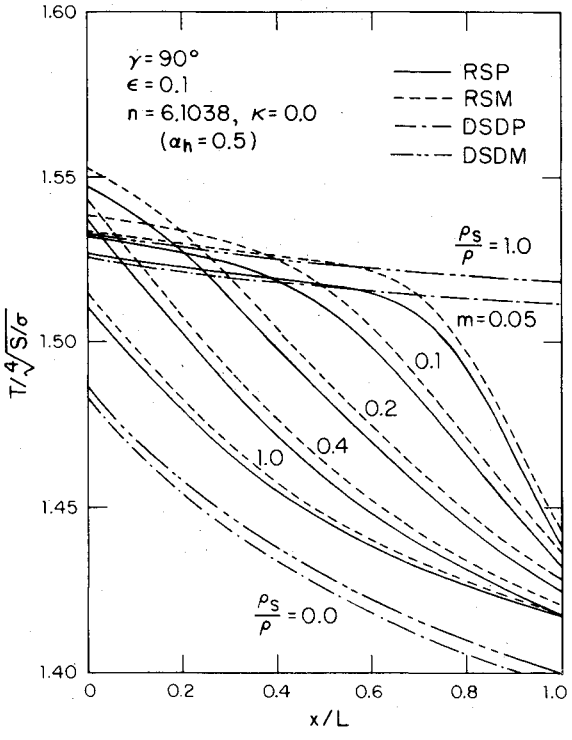

Fig. 5 Equilibrium temperature for $\epsilon = 0.1$, $\alpha_h = 0.5$.

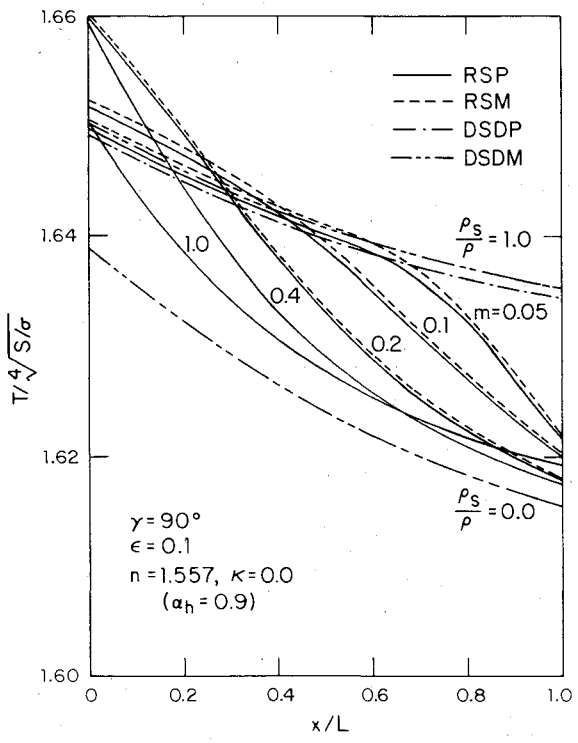

Fig. 6 Equilibrium temperature for $\epsilon = 0.1$, $\alpha_h = 0.9$.

and only a brief explanation is given here. The distributions attain maxima at the common edge and decrease monotonically as the outer edge is approached. Equilibrium temperatures increase with decreasing hemispherical emittance and increasing hemispherical absorptance and exhibit a larger dependency on hemispherical absorptance. As rms slope increases, equilibrium temperatures at the common edge increase up to an rms slope value of approximately 0.2 and then decrease. However, for $\alpha_h = 0.1$, the highest temperatures occur when $m = 1.0$. Equilibrium temperatures continuously decrease as rms slope increases for spatial points near the midpoint of the plates and are nearly insensitive to rms slopes greater than 0.05 at the outer edge.

Included on each figure are equilibrium temperature distributions for the rough surface property model based on the mixed component of bidirectional reflectance (RSM) and for smooth surface directional dependent specular plus diffuse property models with polarization (DSDP) and with mixed component (DSDM). For the latter two models, results are illustrated for diffuse ($\rho_s/\rho = 0.0$) and specular ($\rho_s/\rho = 1.0$) reflection of solar energy. In all instances, distributions based on the mixed component are higher than those evaluated from the polarized components. Distributions for the RSM model are in general agreement with those based on the more extensive RSP model. The maximum difference between these two models occurs in Fig. 5 where $\epsilon = 0.1$ and $\alpha_h = 0.5$ with $m = 0.05$. The error is less than 0.4%, which translates into a temperature difference of approximately 4 K for $S = 1300$ W/m^2, where the common edge temperature is 590 K for the RSP results. The influence of directional dependency of roughness element wall specular reflectance as contained in the RSM model is evaluated later. For spatial positions between the common edge and the midpoint of the plates, results for DSDP and DSDM models with $\rho_s/\rho = 1.0$ are in agreement with the corresponding results for the RSP and RSM models when $m = 0.05$. At the outer edge, however, rough surface results for $m = 0.05$ are lower than smooth surface results with a maximum difference of 7% found in Fig. 4 when $\epsilon = 0.1$ and $\alpha_h = 0.1$. The diffuse results where $\rho_s/\rho = 0.0$ in the DSDP and DSDM models are always lower than the rough surface model results and smooth surface

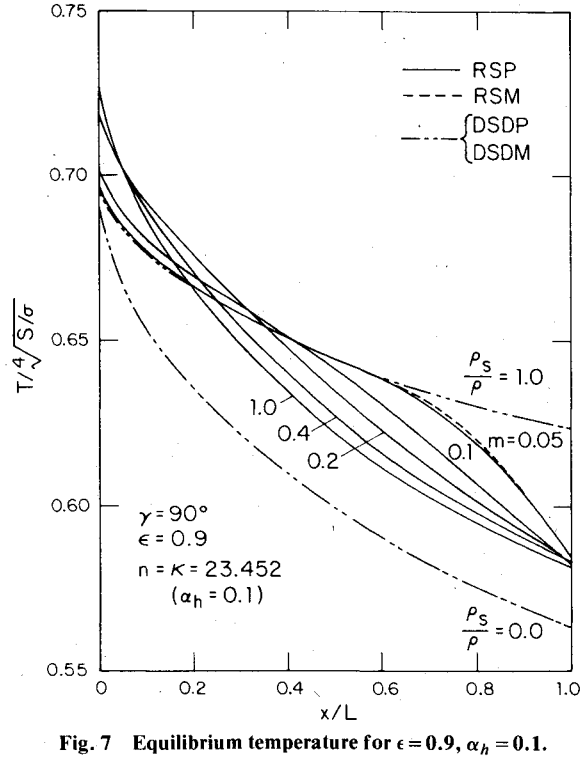

Fig. 7 Equilibrium temperature for $\epsilon = 0.9$, $\alpha_h = 0.1$.

results with specular reflection. Even the distributions for the roughest surface considered where $m = 1.0$ are not represented adequately by distributions for diffuse reflection except for the higher values of hemispherical absorptance. Furthermore, as in agreement with other studies,[3,5,6,8] the limiting cases of diffuse and specular reflection with directional effects accounted for do not bracket the rough surface results.

The influence of directional properties is examined by reference to Figs. 9 and 10 where equilibrium temperature distributions for hemispherical emittance of 0.1 are presented for hemispherical absorptances of 0.1 and 0.9, respectively. In

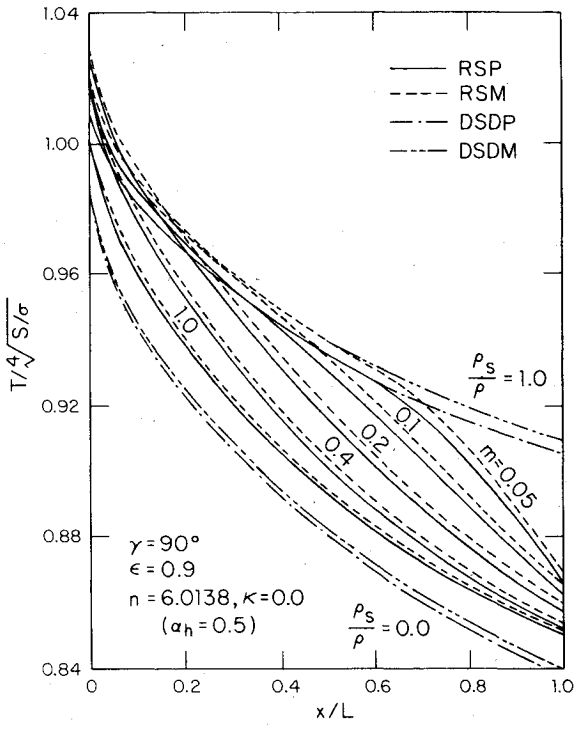

Fig. 8 Equilibrium temperature for $\epsilon = 0.9$, $\alpha_h = 0.5$.

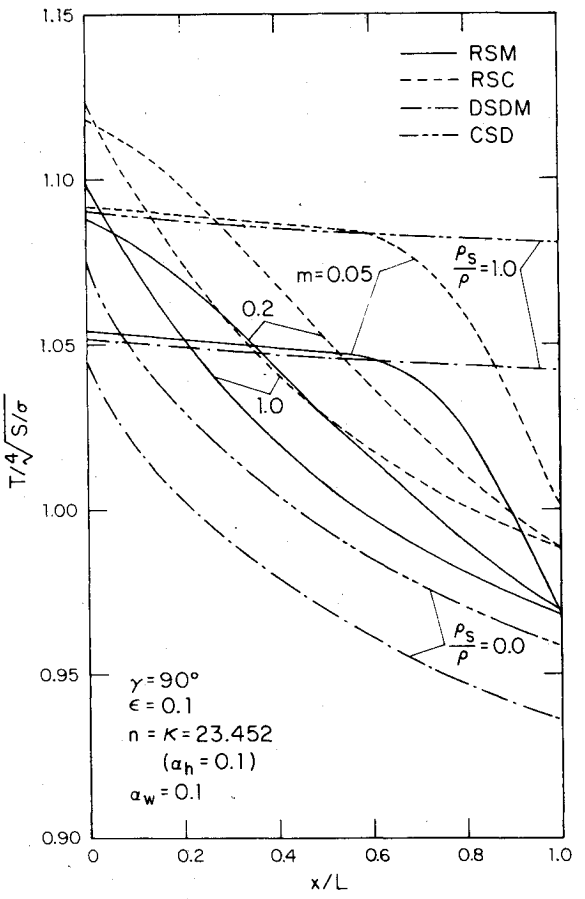

Fig. 9 Comparisons with constant properties for $\epsilon = 0.1$, $\alpha_h = 0.1$.

view of the success of the RSM model in predicting results for the RSP model, distributions for the RSM model are compared with those assuming a constant roughness element wall specular reflectance as denoted by RSC. In addition, results are included for the DSDM and CSD models for specular and

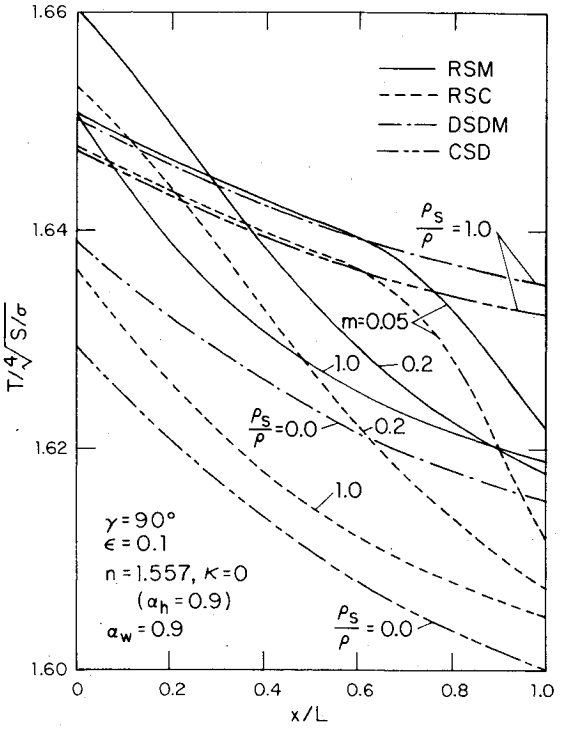

Fig. 10 Comparisons with constant properties for $\epsilon = 0.1$, $\alpha_h = 0.9$.

diffuse reflection. For low values of hemispherical absorptance (0.1), constant property models (RSC and CSD) predict higher equilibrium temperatures in comparison with the directional property models (RSM and DSDM). The maximum difference occurs for slightly rough surfaces where the error is approximately 4%. For high values of hemispherical absorptance (0.9), constant property model results underestimate those for the directional property models. However, these errors are not severe in view of the magnitudes and differences shown in Fig. 10.

Conclusions

An analysis was developed to examine polarization and surface roughness effects on equilibrium temperature for interacting adiabatic surfaces uniformly irradiated by a solar flux. A semigray spectral model was employed to account for radiation property differences between the solar spectral interval and wavelengths of surface or thermal emission. The surfaces are composed of V-shaped roughness elements with randomly distributed included angles as specified by root-mean-square slope. Roughness element walls are specularly reflecting with directional dependent parallel and perpendicular components of reflectance evaluated from electromagnetic theory. For thermal emission, the surfaces are considered to be diffusely emitting and specularly reflecting with a constant specular reflectance. Results for other models based on the mixed component of reflectance are compared with the polarized model results. In addition, model results for constant roughness element wall specular reflectance are reported. Smooth surface results are examined for directional dependent and independent properties where limiting cases of diffuse and specular reflection are considered.

Results presented illustrate that polarization effects are unimportant for the considered system of interacting surfaces. Furthermore, equilibrium temperature distributions derived from a rough surface property model with polarization are represented adequately by those for a rough surface property model based on the mixed component of bidirectional reflectance. Rough surface equilibrium temperature distributions are not bounded by directional dependent smooth surface results with diffuse and specular

reflection. Constant property model results overestimate directional dependent rough surface results for low hemispherical solar absorptances and underpredict for high hemispherical solar absorptances.

Acknowledgment

This study was supported in part by the National Science Foundation Grant CME-7921214.

References

[1]Smith, T. F. and Nichols, K. E., "Effects of Polarization on Bidirectional Reflectance of a One-Dimensional Randomly Rough Surface," AIAA *Progress in Astronautics and Aeronautics: Spacecraft Radiative Transfer and Temperature Control,* Vol. 83, edited by F. E. Horton, AIAA, New York, 1982, pp. 3-21.

[2]Smith, T. F. and Hering, R. G., "Bidirectional Reflectance of a Randomly Rough Surface," AIAA *Progress in Astronautics and Aeronautics: Fundamentals of Spacecraft Thermal Design,* Vol. 29, edited by J. W. Lucas, MIT Press, Cambridge, Mass., 1972, pp. 69-85.

[3]Houchens, A. F. and Hering, R. G., "Surface Roughness Effects on Equilibrium Temperatures," AIAA *Progress in Astronautics and Aeronautics: Thermal Control and Radiation,* Vol. 31, edited by C. L. Tien, MIT Press, Cambridge, Mass., 1973, pp. 435-453.

[4]Beckmann, P. and Spizzichino, A., *The Scattering of Electromagnetic Waves,* Macmillan, New York, 1963.

[5]Hering, R. G. and Smith, T. F., "Surface Roughness Effects on Equilibrium Temperature of Interacting Surfaces," *Journal of Spacecraft and Rockets,* Vol. 8, April 1971, pp. 367-372.

[6]Smith, T. F., "Equilibrium Temperature for Interacting Rough Surfaces," AIAA *Progress in Astronautics and Aeronautics: Heat Transfer with Thermal Control Applications,* Vol. 39, edited by M. Yovanovich, MIT Press, Cambridge, Mass., 1975, pp. 261-272.

[7]Hering, R. G. and Smith, T. F., "Apparent Radiation Properties of a Rough Surface," AIAA *Progress in Astronautics and Aeronautics—Thermophysics: Applications to Thermal Design of Spacecraft,* Vol. 23, edited by J. T. Bevans, Academic Press, 1970, pp. 337-361.

[8]Houchens, A. F. and Hering, R. G., "Directional Property Effects on Radiant Heat Transfer and Equilibrium Temperatures," AIAA *Progress in Astronautics and Aeronautics: Fundamentals of Spacecraft Thermal Design,* Vol. 29, edited by J. W. Lucas, MIT Press, Cambridge, Mass., 1972, pp. 243-268.

[9]Hering, R. G. and Smith T. F., "Surface Radiation Properties from Electromagnetic Theory," *International Journal of Heat and Mass Transfer,* Vol. 11, Oct. 1968, pp. 1567-157l.

[10]Hering, R. G., "Radiative Heat Exchange and Equilibrium Surface Temperature in a Space Environment," *Journal of Spacecraft and Rockets,* Vol. 5, Jan. 1968, pp. 47-54.

[11]Edwards, D. K. and Bevans, J. T., "Effect of Polarization on Spacecraft Radiation Heat Transfer," *AIAA Journal,* Vol. 3, July 1965, pp. 1323-1329.

[12]Edwards, D. K. and Tobin, R. D., "Effect of Polarization on Radiant Heat Transfer Through Long Passage," *ASME Journal of Heat Transfer,* Vol. 89C, May 1967, pp. 132-138.

[13]Smith, T. F. and Hering, R. G., "Surface Roughness Effects on Bidirectional Reflectance," AIAA *Progress in Astronautics and Aeronautics: Thermophysics and Spacecraft Thermal Control,* Vol. 35, edited by R. G. Hering, MIT Press, Cambridge, Mass., 1974, pp. 145-165.